Supporting Informations for

Anthracene Derivatives Bearing Thiourea and Glucopyranosyl Groups for the Highly Selective Chiral Recognition of Amino Acids: Opposite Chiral Selectivities from Similar Binding Units

Yun Kyoung Kim,[a] Han Na Lee,[b] N. Jiten Singh,[c] Hee Jung Choi,[a] Jin Ying Xue,[a]

Kwang S. Kim,[c]* Juyoung Yoon[b]* and Myung Ho Hyun[a]*

[a]*Department of Chemistry, Pusan National University, Pusan 609-735, Korea,* [b]*Division of Nano Science and Department of Chemistry, Ewha Womans University, Seoul 120-750, Korea,* [c]*Center for Superfunctional Materials, Department of Chemistry, Pohang University of Science and Technology, Pohang, 790-784, Korea*

mhhyun@pusan.ac.kr; jyoon@ewha.ac.kr; kim@postech.ac.kr

Experimental Section

General methods. Unless otherwise noted, materials were obtained from commercial suppliers and were used without further purification. Flash chromatography was carried out on silica gel (230-400 mesh). Melting points were measured, and are uncorrected. ^{1}H NMR and ^{13}C NMR spectra were recorded using 300 MHz or 500 MHz NMR. Chemical shifts were expressed in ppm and coupling constants (*J*) in Hz.

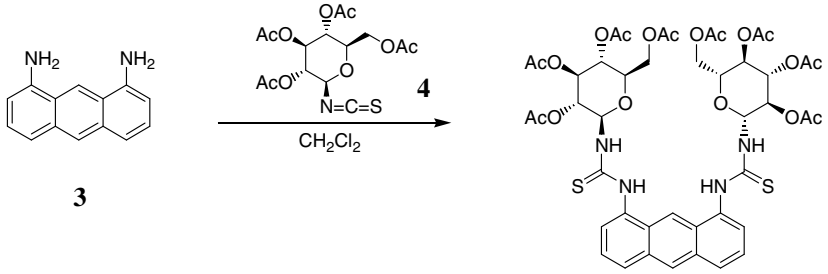

3 **1**

S-Scheme 1. Synthesis of host **1**

Procedure

1. 1,8-Diamino anthracene **3** was synthesized from 1,8-donitroanthraquinone following the reported procedures.[1] To a stirred solution of 1,8-diaminoanthracene **3** (0.1g, 0.48 mmol) in 5 ml of methlyene chloride was added dropwise a solution of 2,3,4,6-tetra-O-acetyl-β-D-glycopyranosyl-isothiocynate(GITC) **4** (0.37 g, 0.95 mmol). The mixture was refluxed for 2 hours under nitrogen gas. The reaction mixture was filtered through a filter paper and the resulting solution was dried with Na_2SO_4. After solvent was evaporated under vacuum, the crude product was purified by flash chromatography (ethyl acetate: hexane: methanol= 1:1:0.1) to afford the product **1** (0.22 g, 0.22 mmol, 46 %) as a brown solid: mp. 162-164 ^{o}C; $[\alpha]_D^{16}$ -29.5° (*c* = 0.1, $CHCl_3$); ^{1}H-NMR (acetone-d_6, ppm) δ 1.94 (s, 12H), 1.96 (s, 6H), 1.99 (s, 6H), 4.00-4.12 (m, 4H), 4.35 (dd, *J* = 4.8 Hz, 2H), 4.95-5.05 (m, 4H), 5.41 (t, *J* = 9.3 Hz, 2H), 6.01 (t, *J* = 9.0 Hz, 2H), 7.53-7.61 (m, 7H), 8.09 (d, *J* = 8.1 Hz, 2H), 8.72 (d, *J* = 16.5 Hz, 2H), 9.73 (s, 1H). ^{13}C-NMR (CD_3CN, ppm) δ 21.0, 20.1, 20.1, 30.1, 30.0, 62.1, 68.7, 71.1, 73.3, 73.5, 83.1, 115.4, 125.7, 128.0, 128.6, 132.9, 134.1, 169.5, 169.6, 170.4, 184.3, 206.2. IR (KBr) cm^{-1} 3356.50, 2929.34, 1752.98, 1536.99, 1370.18, 1230.36, 1038.48, 599.75; HR-ESI-MS *m/z* = 987.2653 $(M + H)^+$, calcd for $C_{44}H_{51}N_4O_{18}S_2$ = 987.2632.

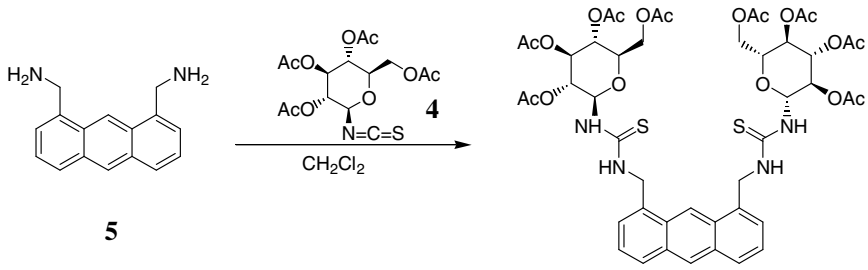

5 **2**

S-Scheme 2. Synthesis of host **2**

Procedure

2. 1,8-Bis(aminomethyl)anthracene **5** was synthesized from 1,8-bis(hydroxymethyl)anthracene following the reported procedure.[2] To a stirred solution of 1,8-bis(aminomethyl)anthracene **5** (0.1g, 0.42 mmol) in 20 ml of methlyene chloride was added dropwise a solution of 2,3,4,6-tetra-O-acetyl-β-D-glycopyranosyl-isothiocynate(GITC) 4 (0.33 g, 0.85 mmol). The mixture was stirred for 1 hour under nitrogen gas at room temperature. Solvent was evaporated under vacuum and the crude product was purified by flash chromatography (ethyl acetate :hexane :methanol = 1:1:0.1) to afford the product **2** (0.30 g, 0.30 mmol, 70 %) as a yellow solid: mp. 160-162 ^{o}C; $[\alpha]_{D}^{16}$ -13.2° (*c*=0.1, $CHCl_3$); ^{1}H-NMR (acetone-d_6, ppm) δ 1.84 (s, 6H), 1.94 (s, 6H), 1.96 (s, 6H), 1.99 (s, 6H), 3.99-4.07 (m, 4H), 4.26 (dd, *J* = 4.5 Hz, 2H), 4.93-5.04 (m, 4H), 5.39 (t, *J* = 9.6 Hz, 2H), 5.49 (d, 4H), 6.00 (t, *J* = 6.9 Hz, 2H), 7.40 (d, *J* = 8.4 Hz, 2H), 7.47 (t, *J* = 7.7 Hz, 2H), 7.57 (d, *J* = 6.9 Hz, 2H), 7.93 (t, 2H), 8.03 (d, *J* = 8.1 Hz, 2H), 8.61 (s, 1H), 8.92 (s, 1H); ^{13}C-NMR (CD_3CN, ppm) δ 20.1, 20.2, 20.2, 46.6, 62.1, 68.6, 71.1, 73.5, 78.5, 82.3, 118.4, 125.4, 125.8, 128.2, 128.4, 129.8, 132.0, 134.4, 170.2, 170.4, 170.6, 171.0, 184.4; IR (KBr) cm^{-1} 3360.35, 2925.34, 1547.59, 1377.89, 1234.22, 1037.52, 600.72; HR-ESI-MS *m/z* = 1015.2987 $(M + H)^+$, calcd for $C_{46}H_{55}N_4O_{18}S_2$ = 1015.2946.

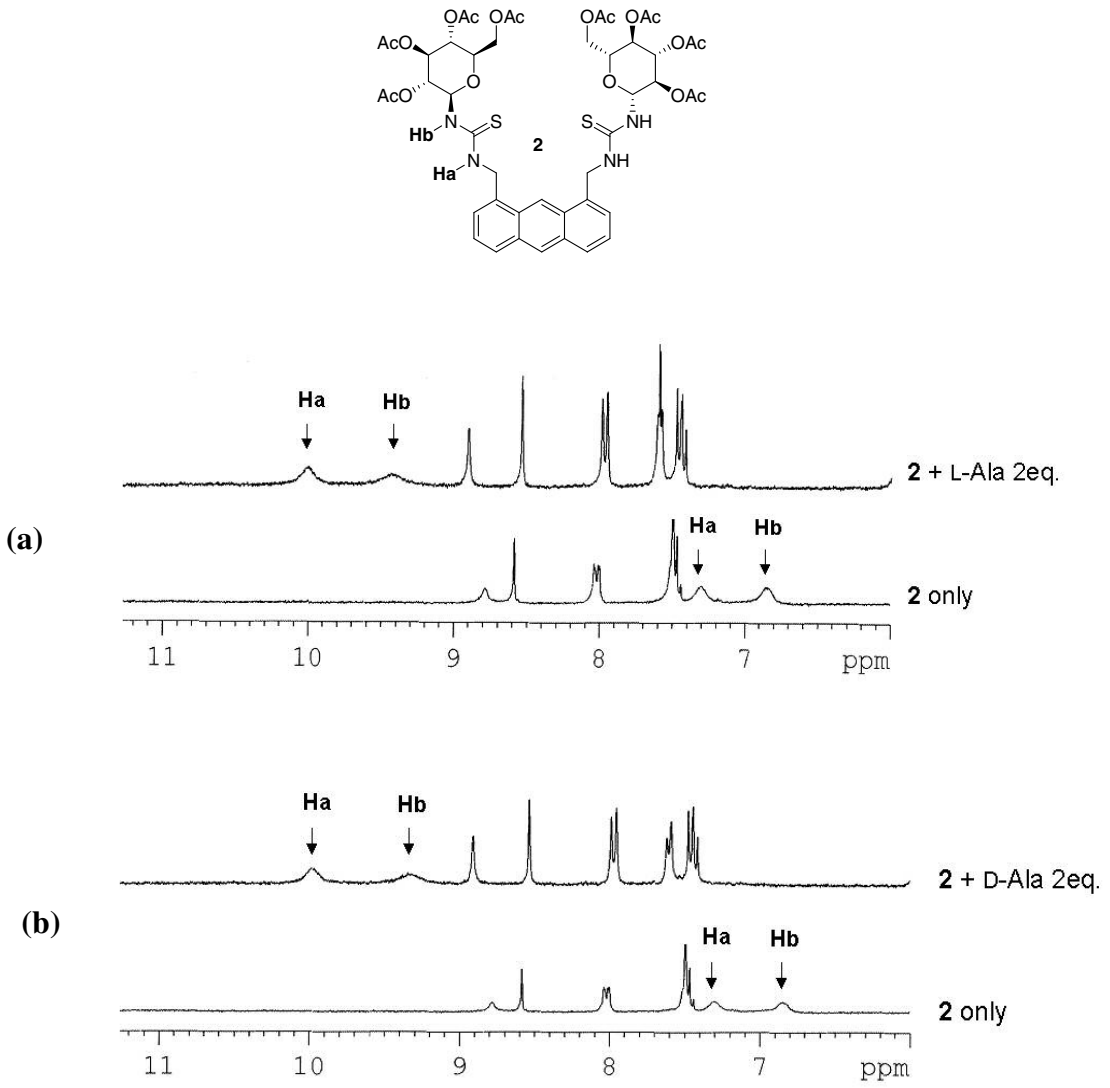

S-Figure 1. (a) Partial ^{1}H NMR spectra (250 MHz) of host **2** upon addition of *t*-Boc-L-alanine (2eq.) in CD_3CN; (b) Partial ^{1}H NMR spectra (250 MHz) of host **2** upon addition of *t*-Boc-D-alanine (2eq.) in CD_3CN.

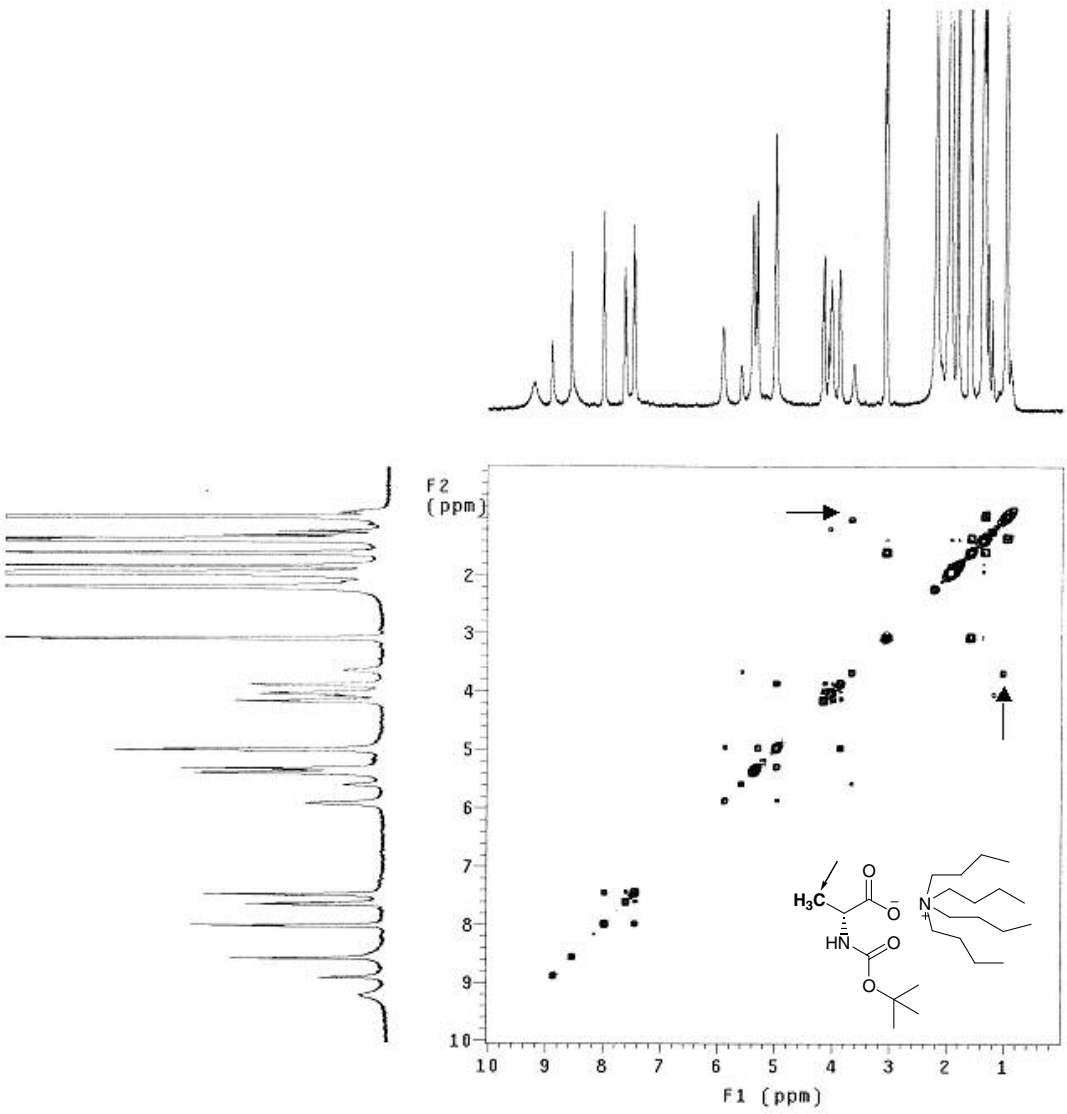

S-Figure 2. ^{1}H-^{1}H COSY 2D NMR spectrum (500 MHz) of host **2** upon addition of t-Boc-L-alanine (1eq.) in CD_3CN (arrow: a cross peak of side chain CH_3 in *t*-Boc-L-alanine)

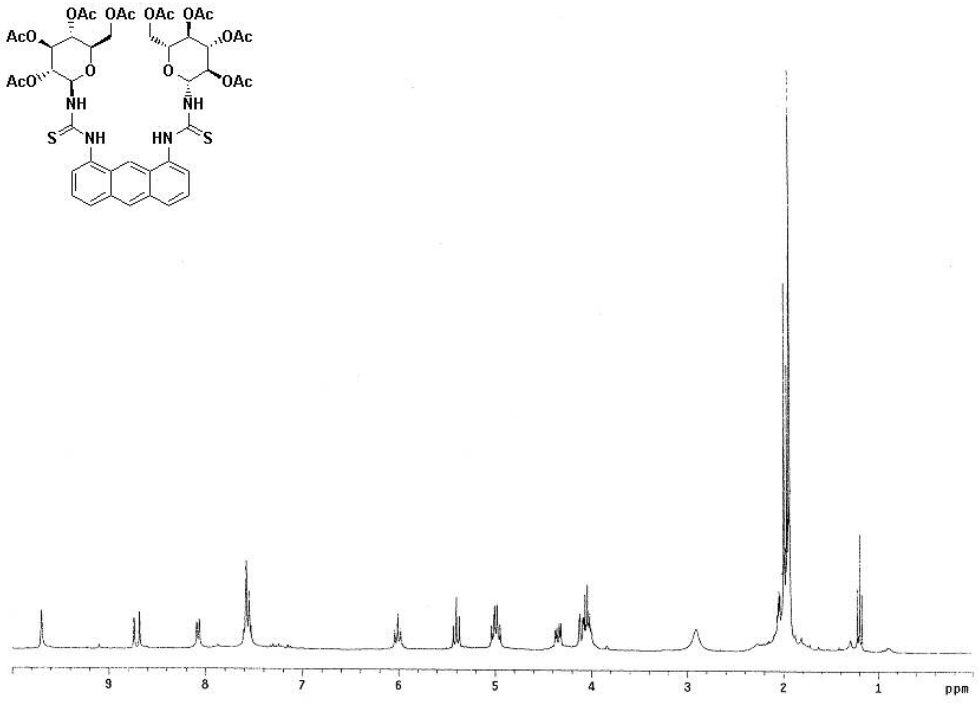

S-Figure 3. ^{1}H NMR (300 MHz) spectrum of compound **1** in acetone-d_6

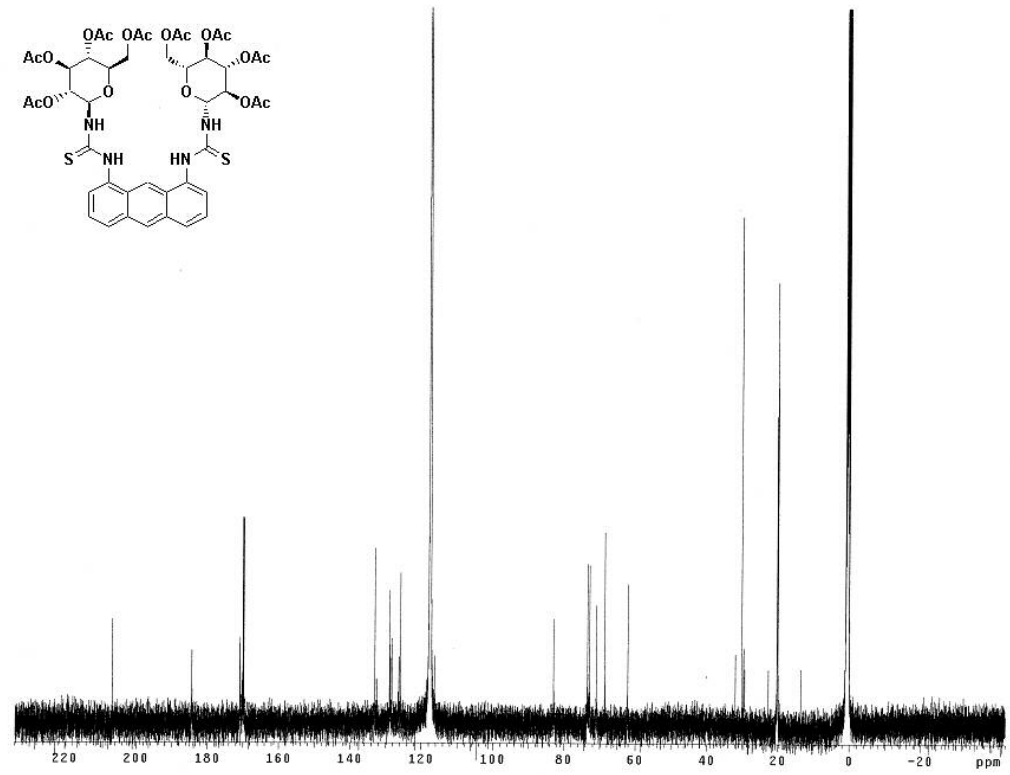

S-Figure 4. ^{13}C NMR (125 MHz) spectrum of compound **1** in CD_3CN

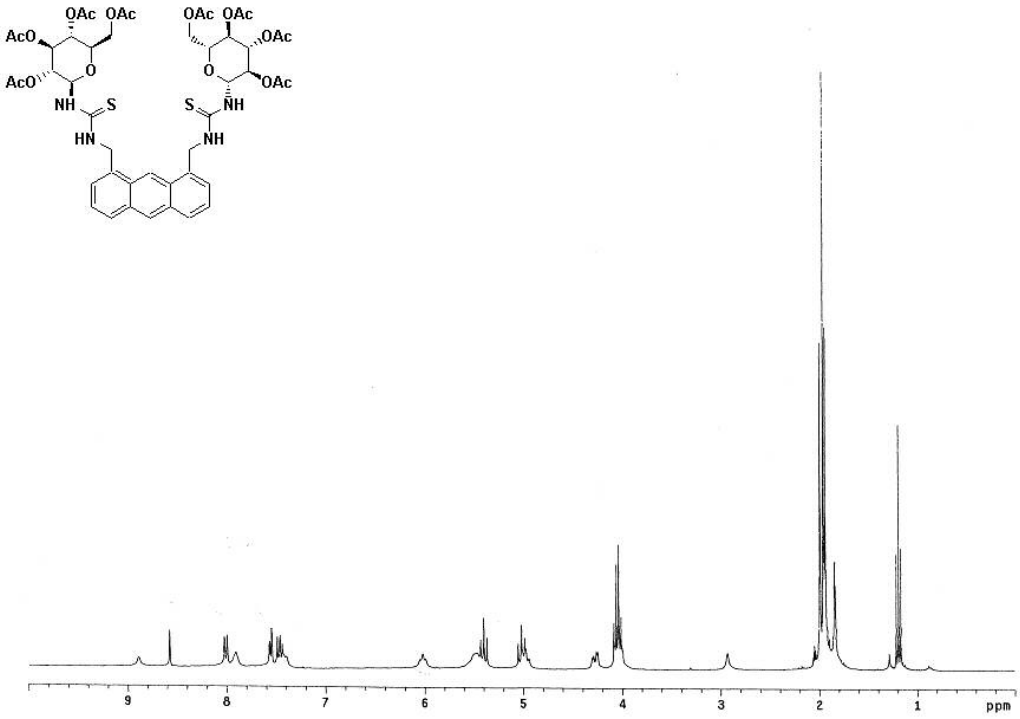

S-Figure 5. ^{1}H NMR (300 MHz) spectrum of compound **2** in acetone-d_6

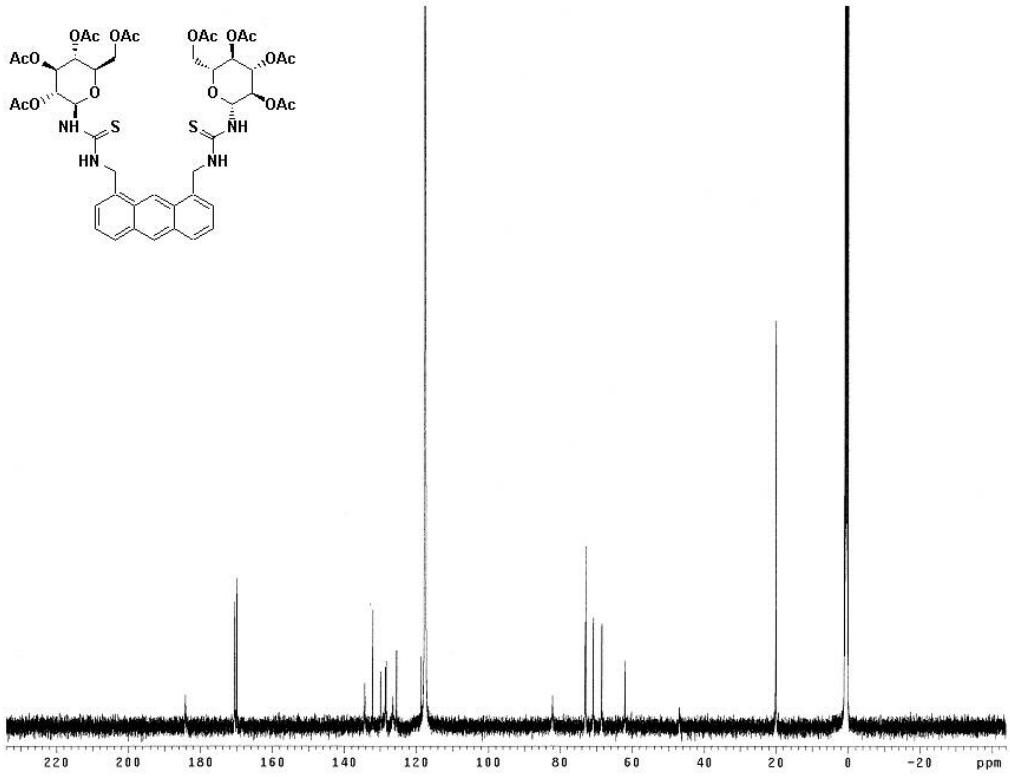

S-Figure 6. ^{13}C NMR (125 MHz) spectrum of compound **2** in CD_3CN

(a)

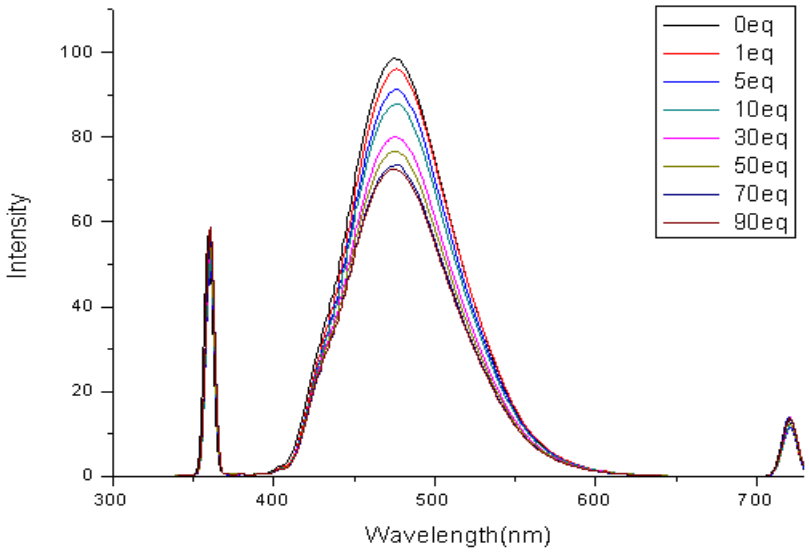

(b)

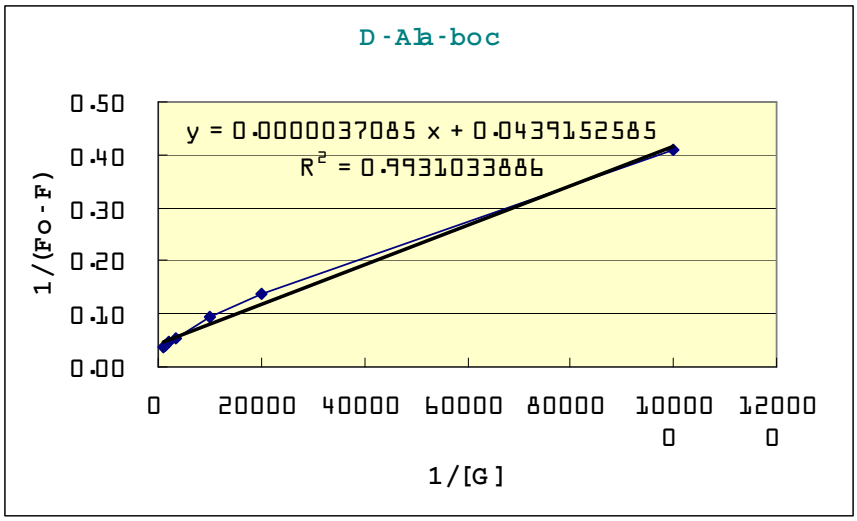

$$K_a = 11841.78\ M^{-1}$$

S-Figure 7. (a) Fluorescent titration spectra of **1** (10 μM) upon addition of *t*-Boc-D-alanine in 100 % CH_3CN (excitation: 360 nm). (b) Benesi-Hildebrand plot of emission spectra of **1** at 360 nm: [1 / (F_0-F)] / [G].

(a)

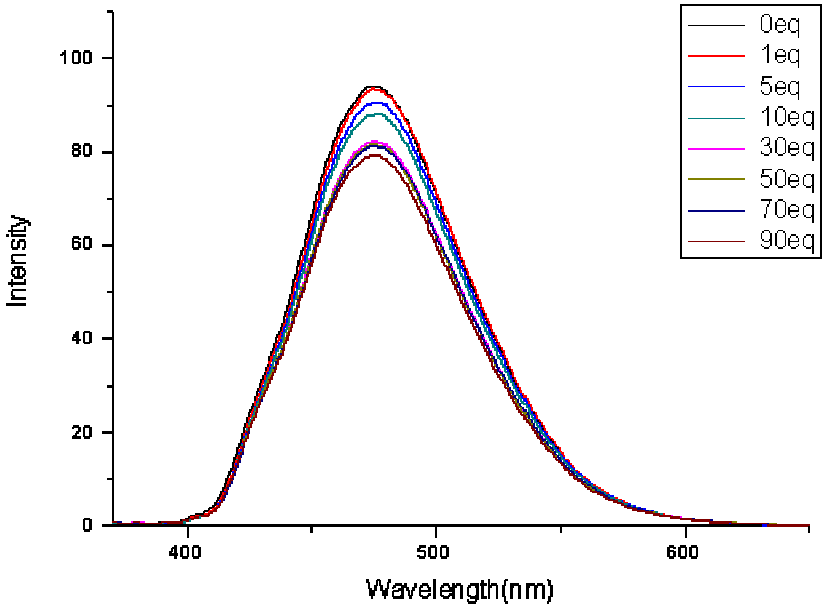

(b)

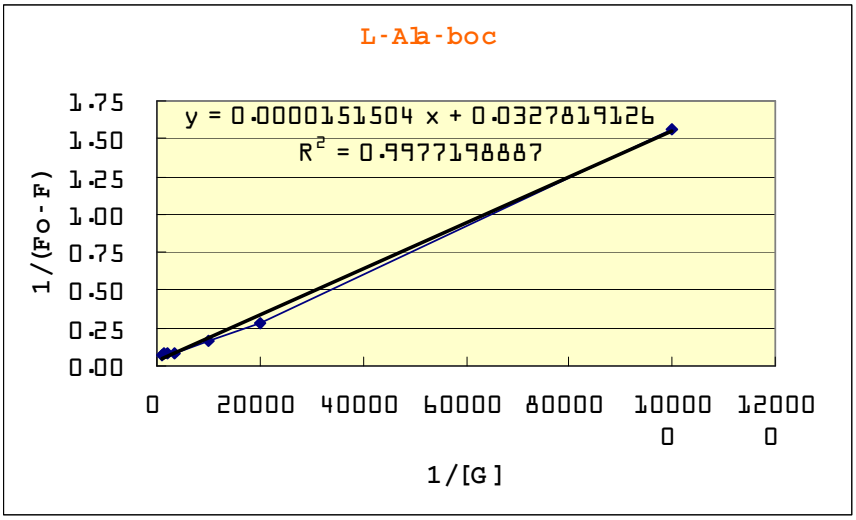

$$K_a = 2163.77\ M^{-1}$$

S-Figure 8. (a) Fluorescent titration spectra of **1** (10 μM) upon addition of *t*-Boc-L-alanine in 100 % CH_3CN (excitation: 360 nm). (b) Benesi-Hildebrand plot of emission spectra of **1** at 360 nm: [1 / (F_0-F)] / [G].

(a)

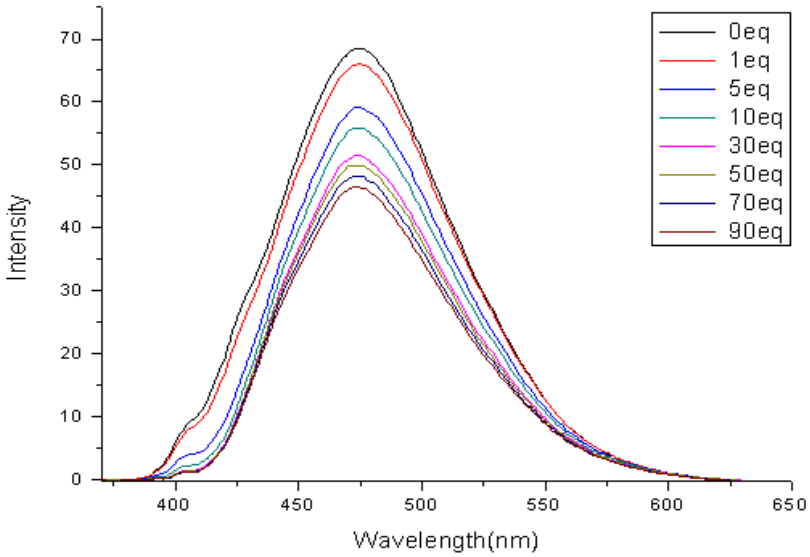

(b)

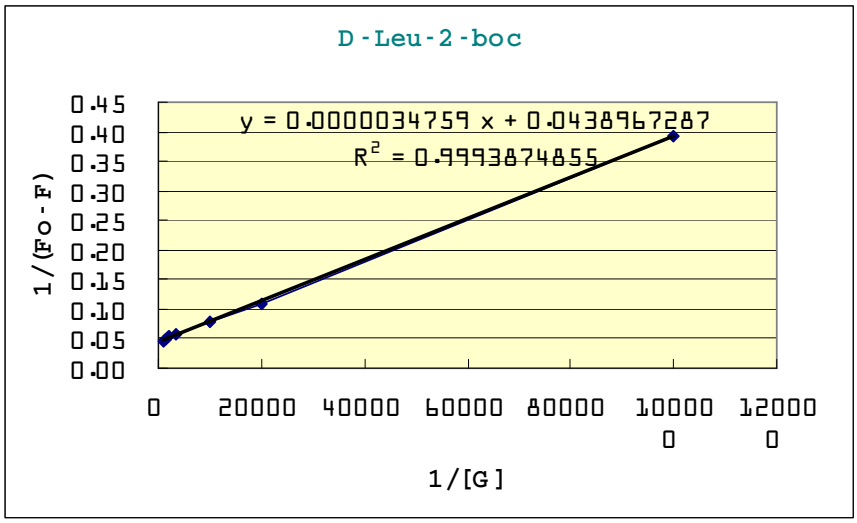

$K_a = 12628.88\ M^{-1}$

S-Figure 9. (a) Fluorescent titration spectra of **1** (10 μM) upon addition of *t*-Boc-D-leucine in 100 % CH_3CN (excitation: 360 nm). (b) Benesi-Hildebrand plot of emission spectra of **1** at 360 nm: [1 / (F_0-F)] / [G].

(a)

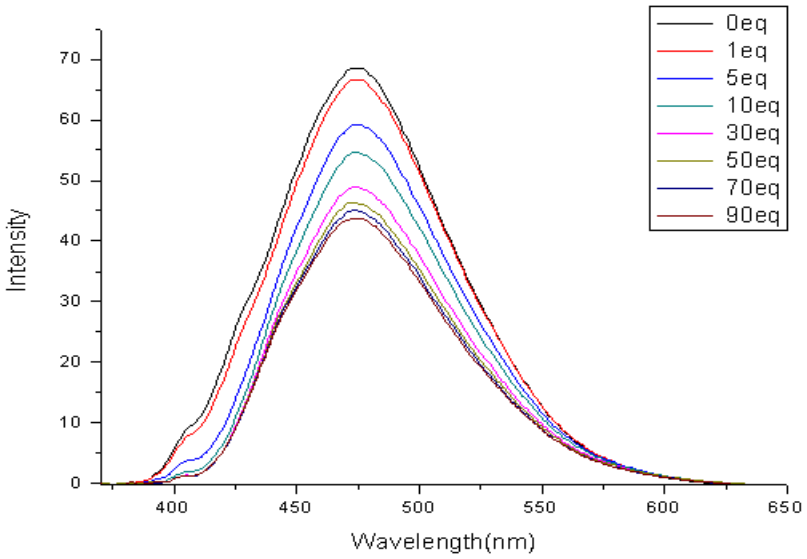

(b)

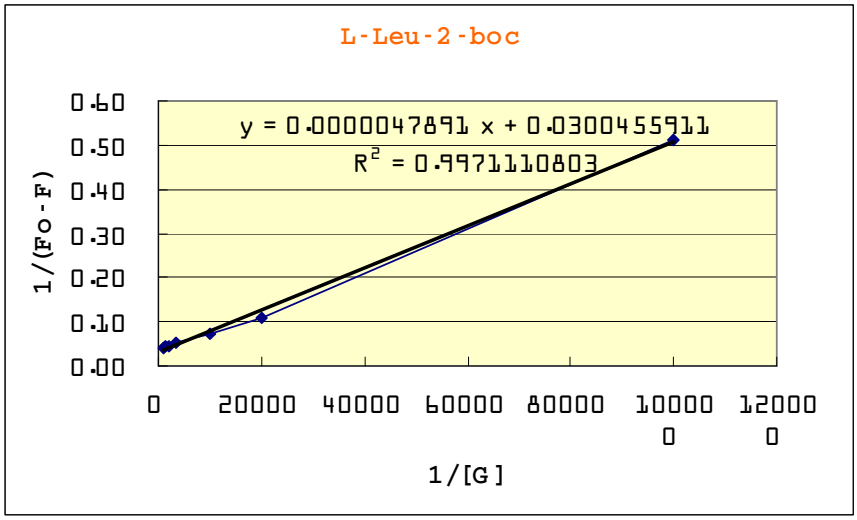

$K_a = 6273.74\ M^{-1}$

S-Figure 10. (a) Fluorescent titration spectra of **1** (10 μM) upon addition of *t*-Boc-L-leucine in 100 % CH_3CN (excitation: 360 nm). (b) Benesi-Hildebrand plot of emission spectra of **1** at 360 nm: [1 / (F_0-F)] / [G].

(a)

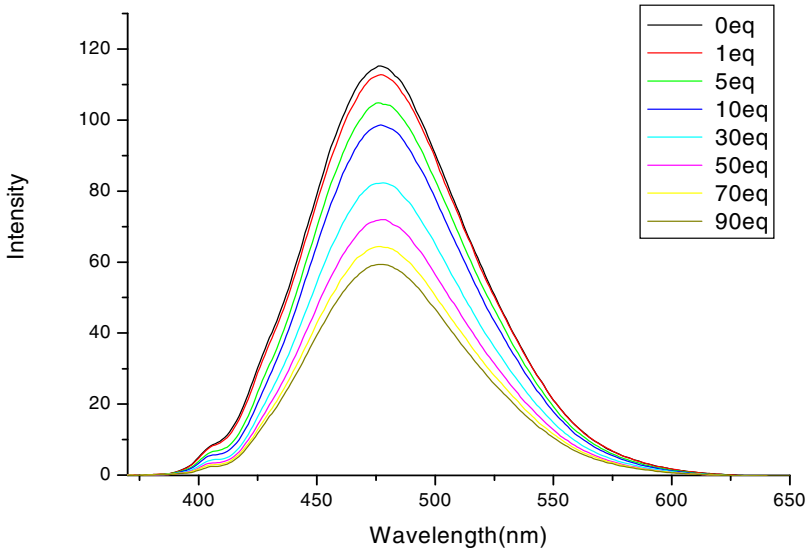

(b)

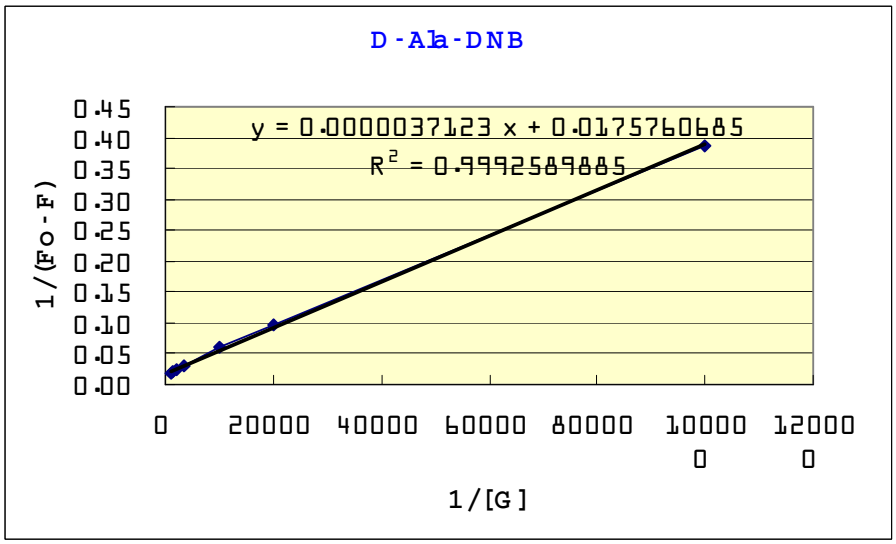

$K_a = 4734.55\ M^{-1}$

S-Figure 11. (a) Fluorescent titration spectra of **1** (10 μM) upon addition of DNB-D-alanine in 100 % CH_3CN (excitation: 360 nm). (b) Benesi-Hildebrand plot of emission spectra of **1** at 360 nm: [1 / (F_0-F)] / [G].

(a)

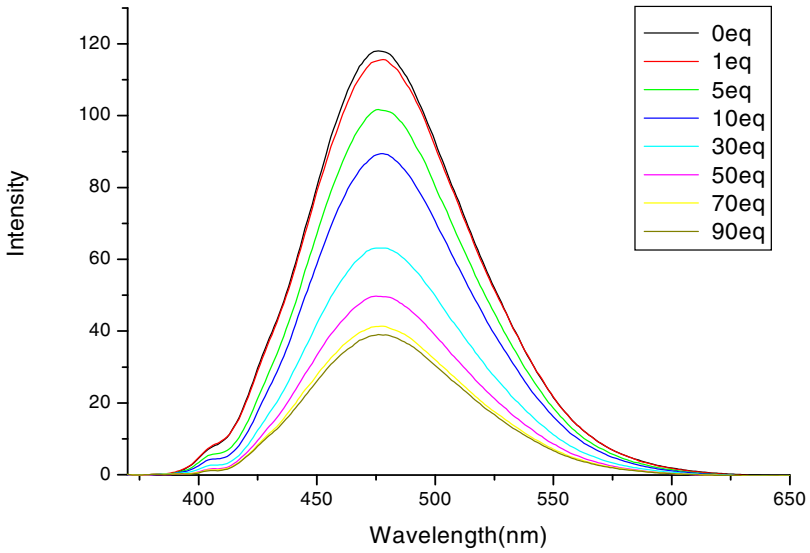

(b)

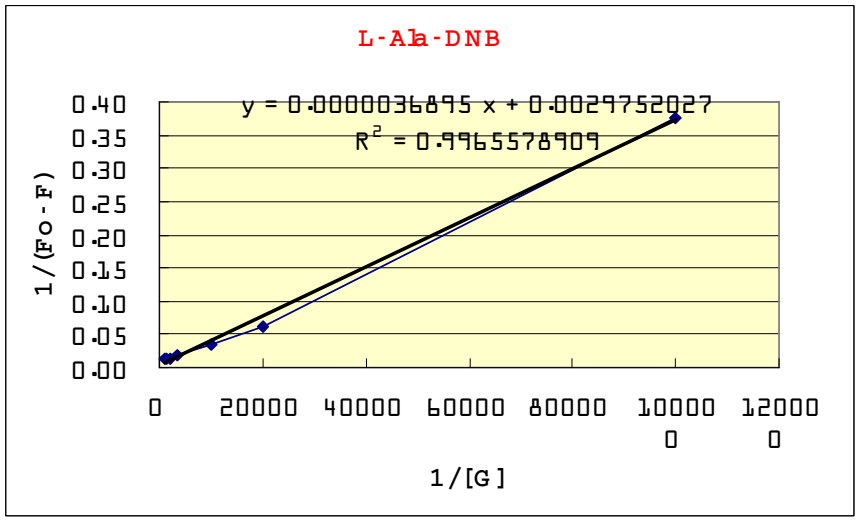

$K_a = 806.40\ M^{-1}$

S-Figure 12. (a) Fluorescent titration spectra of **1** (10 μM) upon addition of DNB-L-alanine in 100 % CH_3CN (excitation: 360 nm). (b) Benesi-Hildebrand plot of emission spectra of **1** at 360 nm: [1 / (F_0-F)] / [G].

(a)

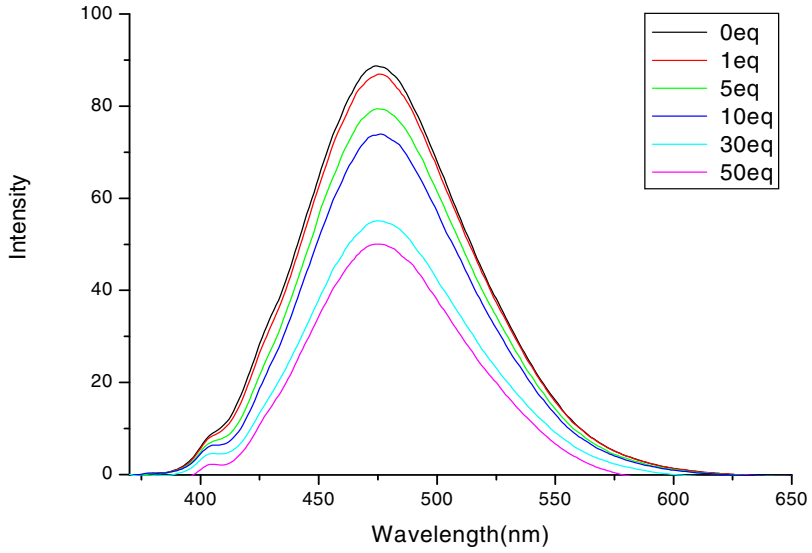

(b)

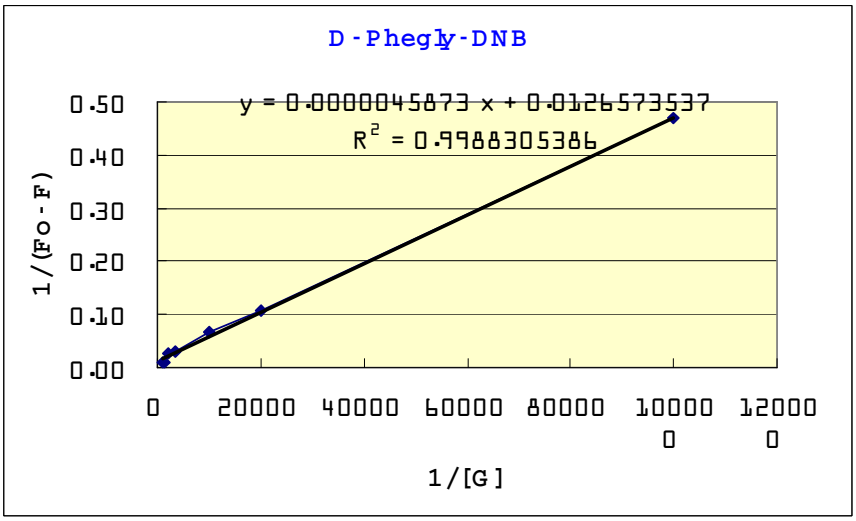

$$K_a = 2759.22\ M^{-1}$$

S-Figure 13. (a) Fluorescent titration spectra of **1** (10 μM) upon addition of DNB-D-Phenylglycine in 100 % CH_3CN (excitation: 360 nm). (b) Benesi-Hildebrand plot of emission spectra of **1** at 360 nm: [1 / (F_0-F)] / [G].

(a)

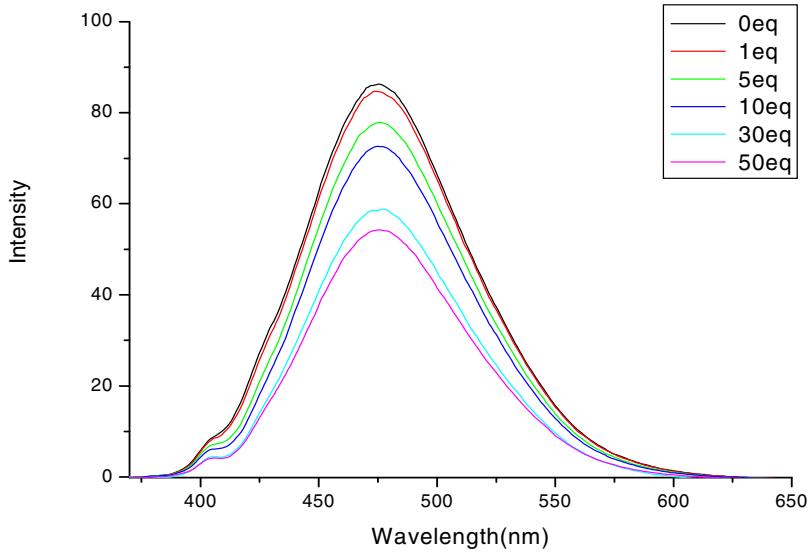

(b)

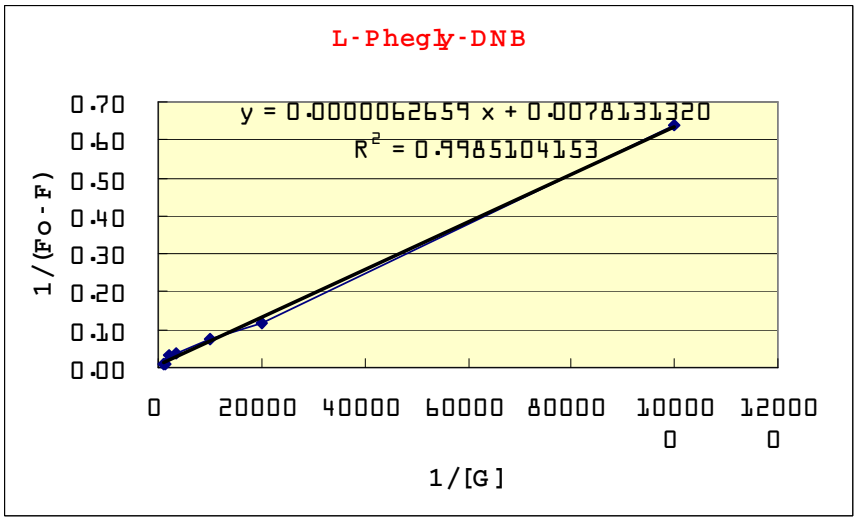

$$K_a = 1246.93\ M^{-1}$$

S-Figure 14. (a) Fluorescent titration spectra of **1** (10 μM) upon addition of DNB-L-Phenylglycine in 100 % CH_3CN (excitation: 360 nm). (b) Benesi-Hildebrand plot of emission spectra of **1** at 360 nm: [1 / (F_0-F)] / [G].

(a)

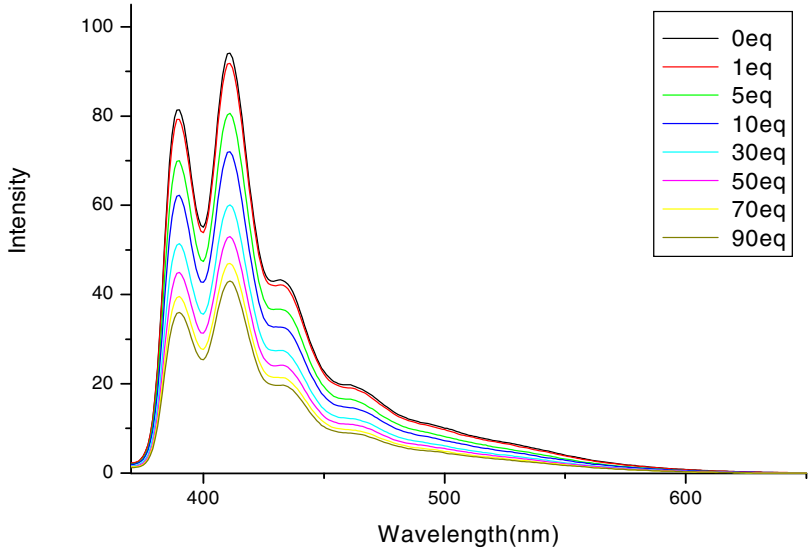

(b)

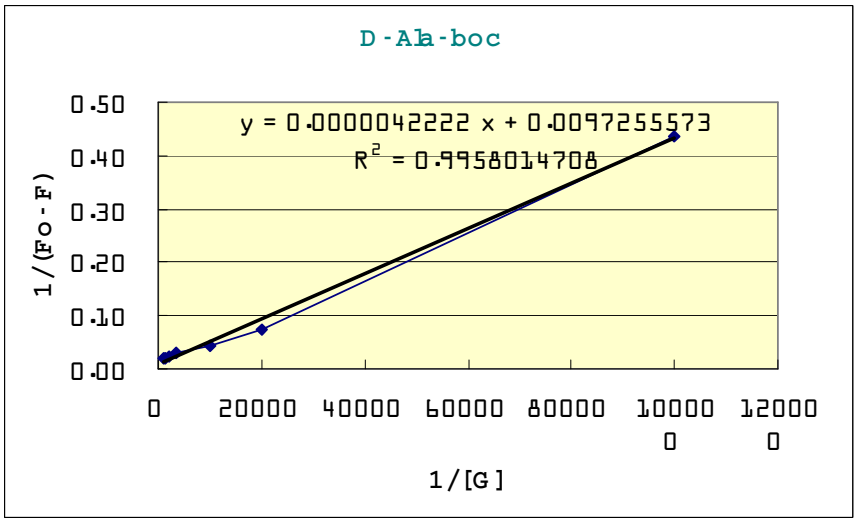

$$K_a = 2303.43\ M^{-1}$$

S-Figure 15. (a) Fluorescent titration spectra of **2** (10 μM) upon addition of *t*-Boc-D-alanine in 100 % CH_3CN (excitation: 360 nm). (b) Benesi-Hildebrand plot of emission spectra of **2** at 360 nm: [1 / (F_0-F)] / [G].

(a)

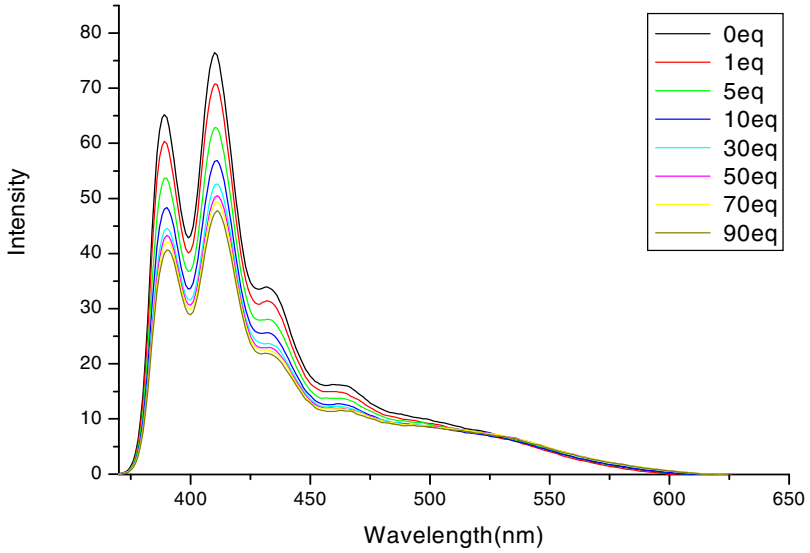

(b)

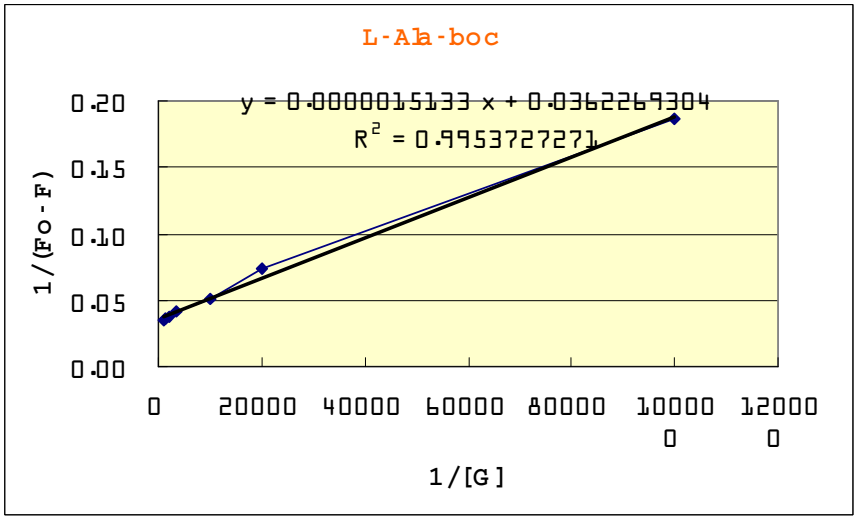

$K_a = 23939.03\ M^{-1}$

S-Figure 16. (a) Fluorescent titration spectra of **2** (10 μM) upon addition of *t*-Boc-L-alanine in 100 % CH_3CN (excitation: 360 nm). (b) Benesi-Hildebrand plot of emission spectra of **2** at 360 nm: [1 / (F_0-F)] / [G].

(a)

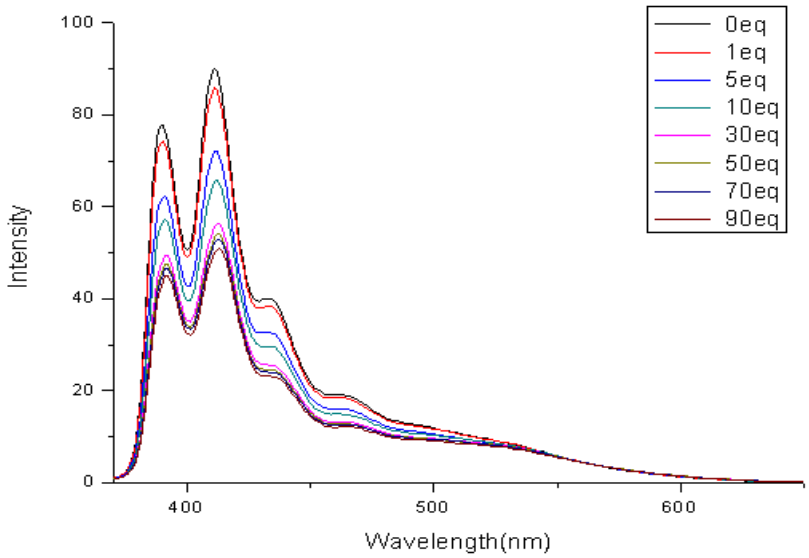

(b)

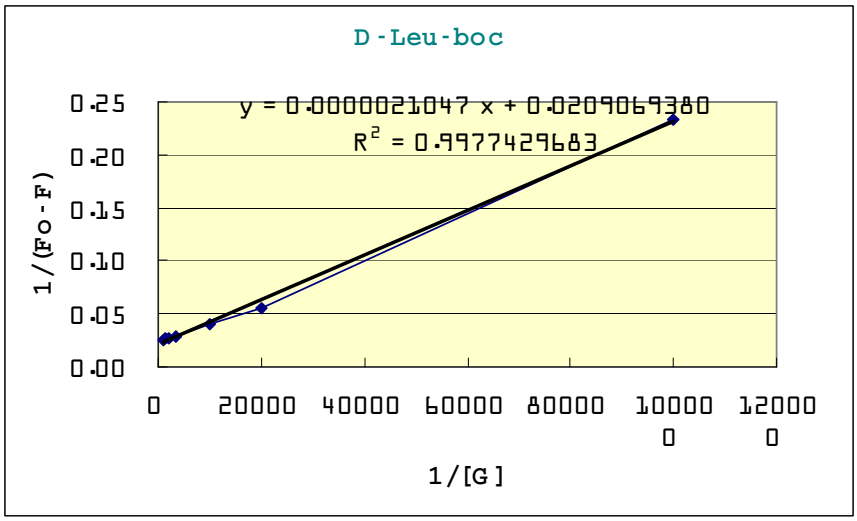

$$K_a = 9933.45\ M^{-1}$$

S-Figure 17. (a) Fluorescent titration spectra of **2** (10 μM) upon addition of *t*-Boc-D-leucine in 100 % CH_3CN (excitation: 360 nm). (b) Benesi-Hildebrand plot of emission spectra of **2** at 360 nm: [1 / (F_0-F)] / [G].

(a)

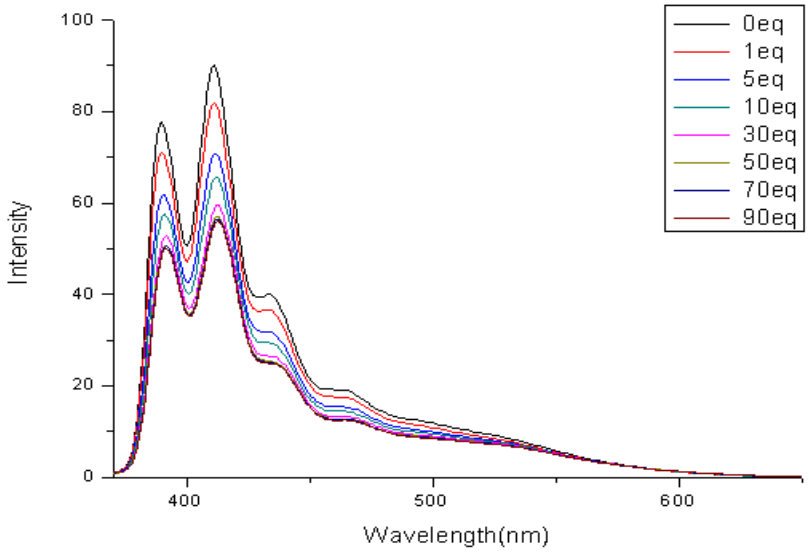

(b)

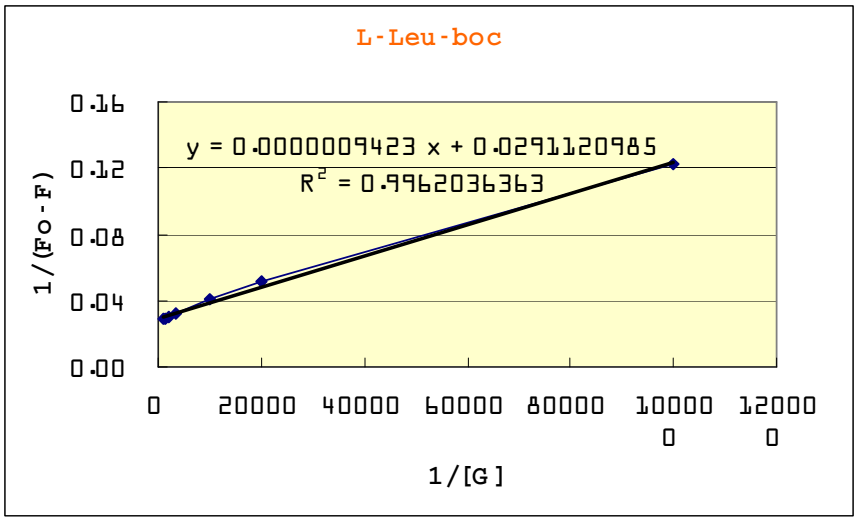

$K_a = 30894.72\ M^{-1}$

S-Figure 18. (a) Fluorescent titration spectra of **2** (10 μM) upon addition of *t*-Boc-D-leucine in 100 % CH_3CN (excitation: 360 nm). (b) Benesi-Hildebrand plot of emission spectra of **2** at 360 nm: [1 / (F_0-F)] / [G].

(a)

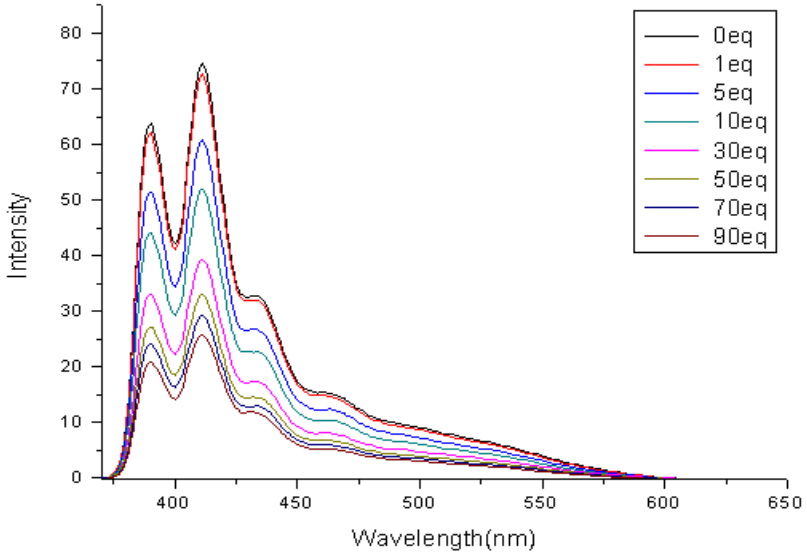

(b)

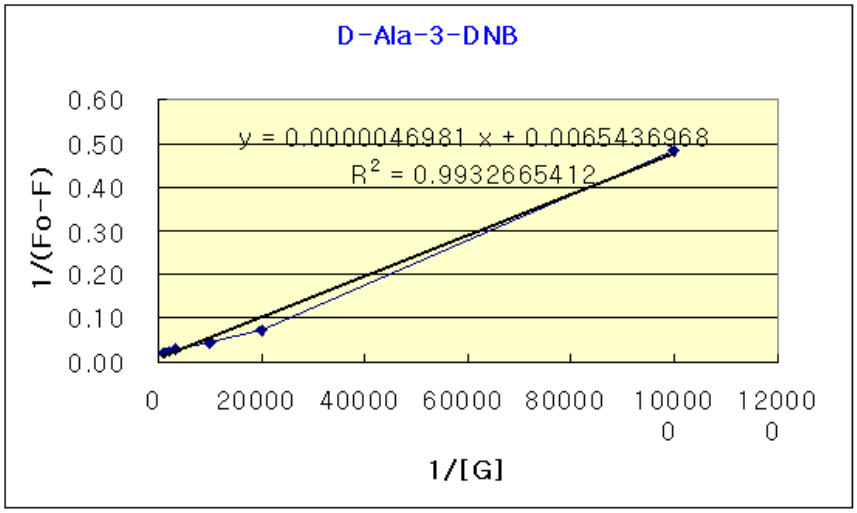

$K_a = 1392.84\ M^{-1}$

S-Figure 19. (a) Fluorescent titration spectra of **2** (10 μM) upon addition of DNB-D-alanine in 100 % CH_3CN (excitation: 360 nm). (b) Benesi-Hildebrand plot of emission spectra of **2** at 360 nm: [1 / (F_0-F)] / [G].

(a)

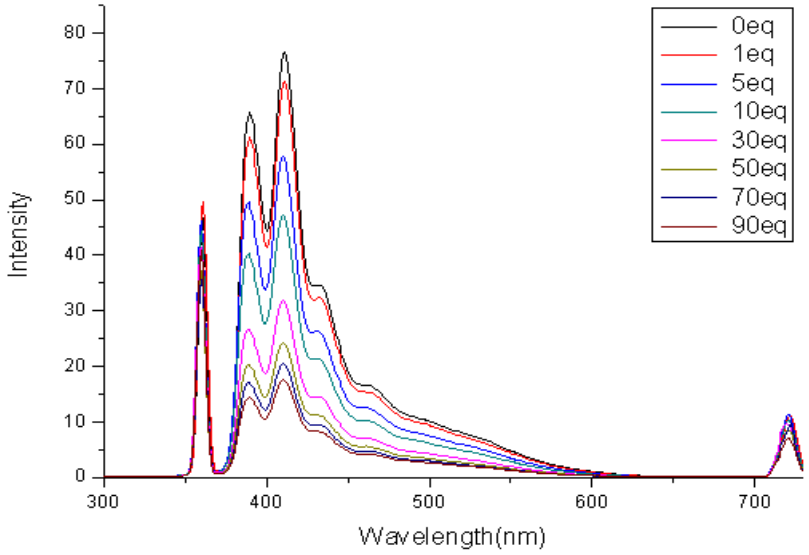

(b)

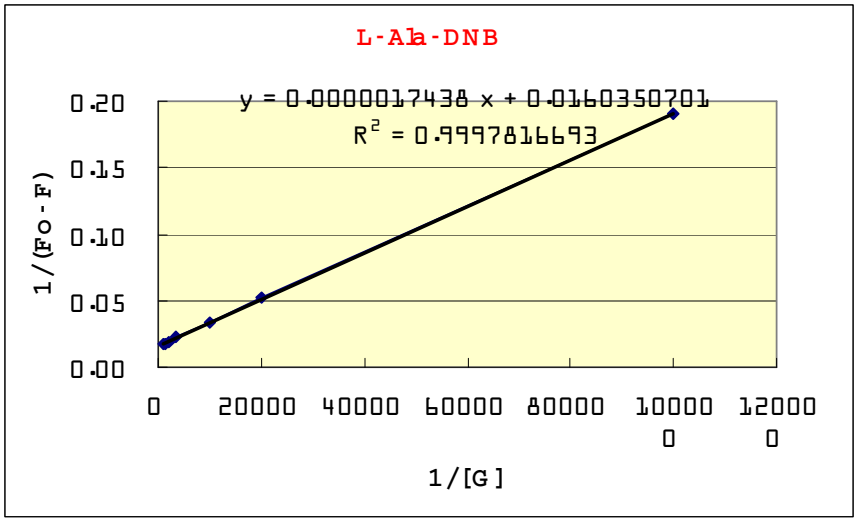

$K_a = 9195.48\ M^{-1}$

S-Figure 20. (a) Fluorescent titration spectra of **2** (10 μM) upon addition of DNB-L-alanine in 100 % CH_3CN (excitation: 360 nm). (b) Benesi-Hildebrand plot of emission spectra of **2** at 360 nm : [1 / (F_0-F)] / [G].

(a)

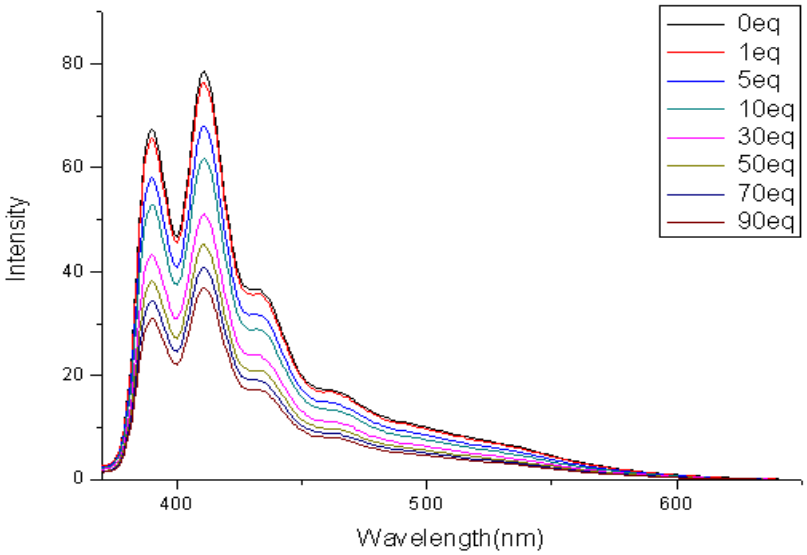

(b)

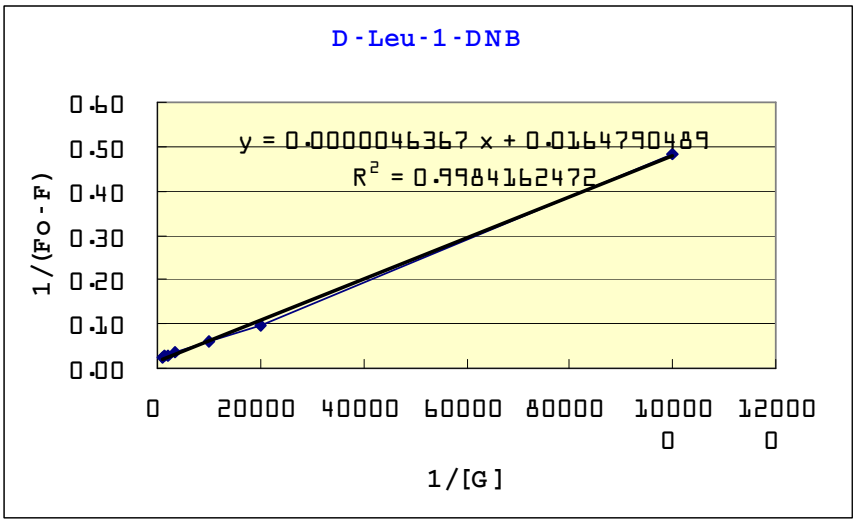

$K_a = 3554.05\ M^{-1}$

S-Figure 21. (a) Fluorescent titration spectra of **2** (10 μM) upon addition of DNB-D-leucine in 100 % CH_3CN (excitation: 360 nm). (b) Benesi-Hildebrand plot of emission spectra of **2** at 360 nm : [1 / (F_0-F)] / [G].

(a)

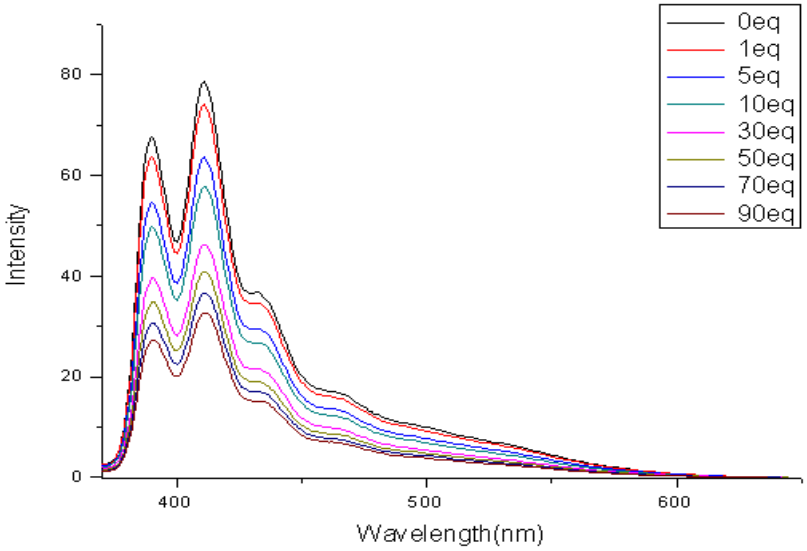

(b)

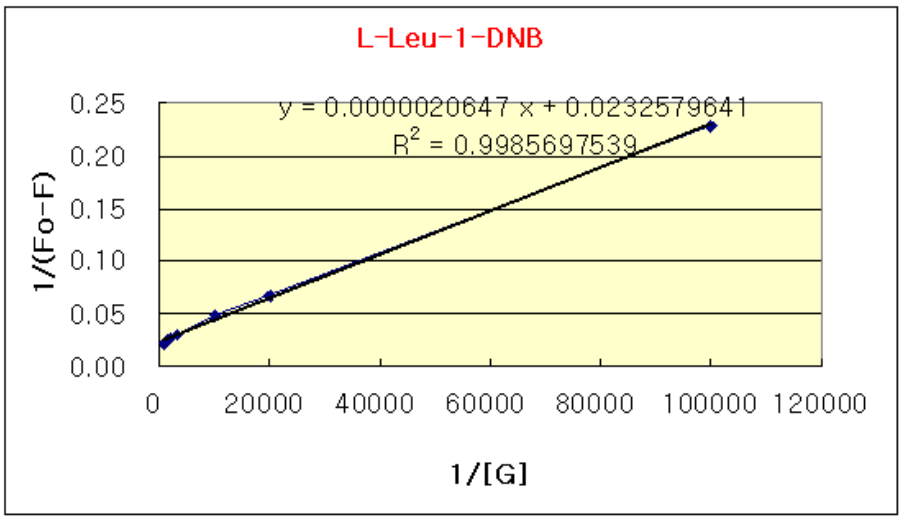

$K_a = 11264.57\ M^{-1}$

S-Figure 22. (a) Fluorescent titration spectra of **2** (10 μM) upon addition of DNB-L-leucine in 100 % CH_3CN (excitation: 360 nm). (b) Benesi-Hildebrand plot of emission spectra of **2** at 360 nm: [1 / (F_0-F)] / [G].

(a)

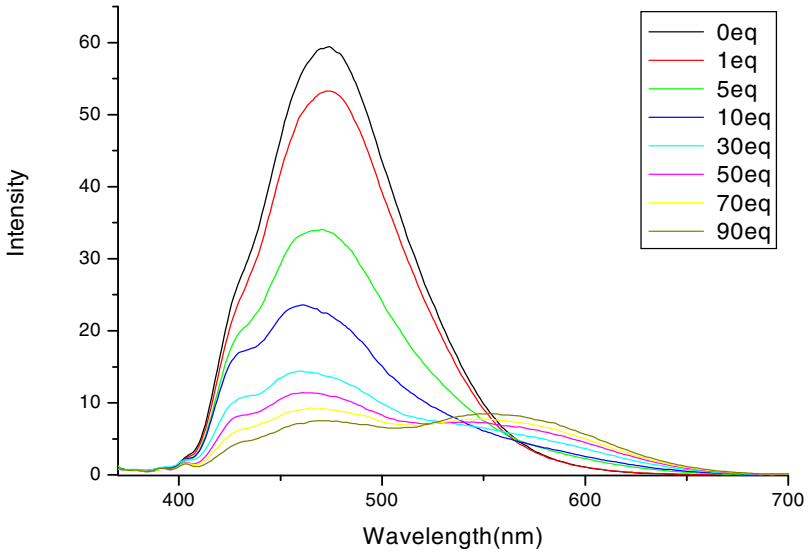

(b)

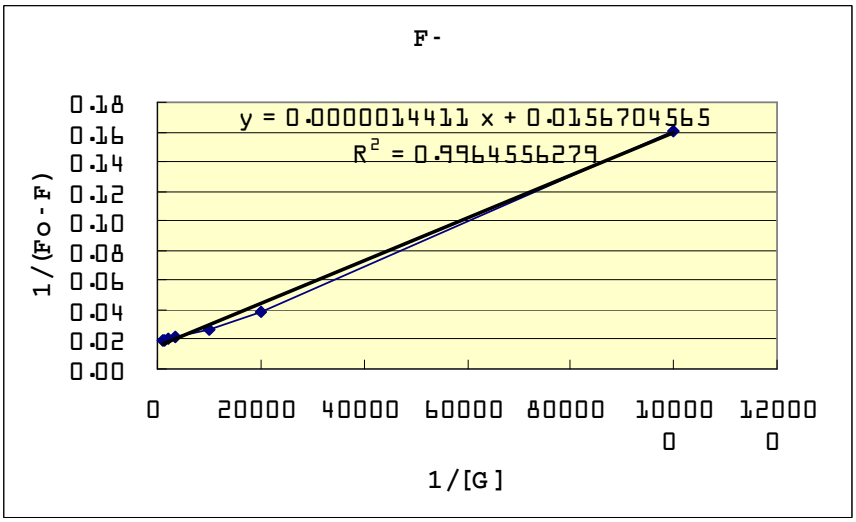

$K_a = 10873.95\ M^{-1}$

S-Figure 23. (a) Fluorescent titration spectra of **1** (10 μM) upon addition of Fluoride ion in 100 % CH_3CN (excitation: 360 nm). (b) Benesi-Hildebrand plot of emission spectra of **1** at 360 nm: [1 / (F_0-F)] / [G].

(a)

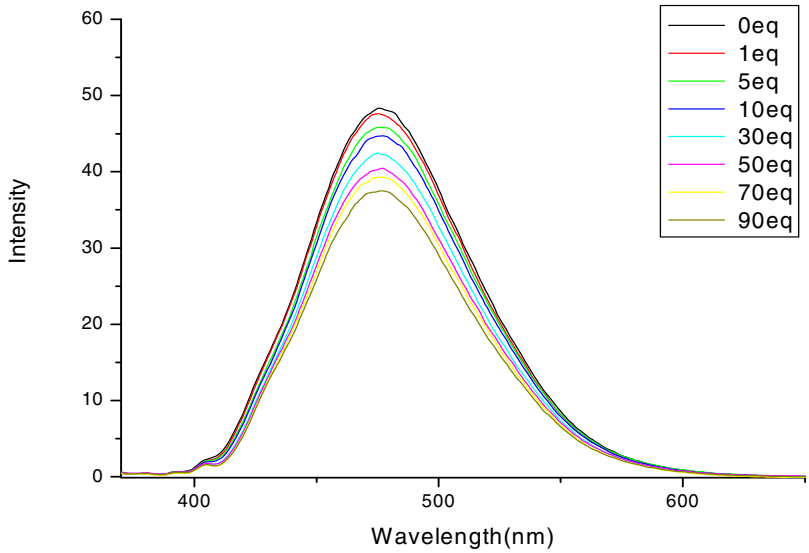

(b)

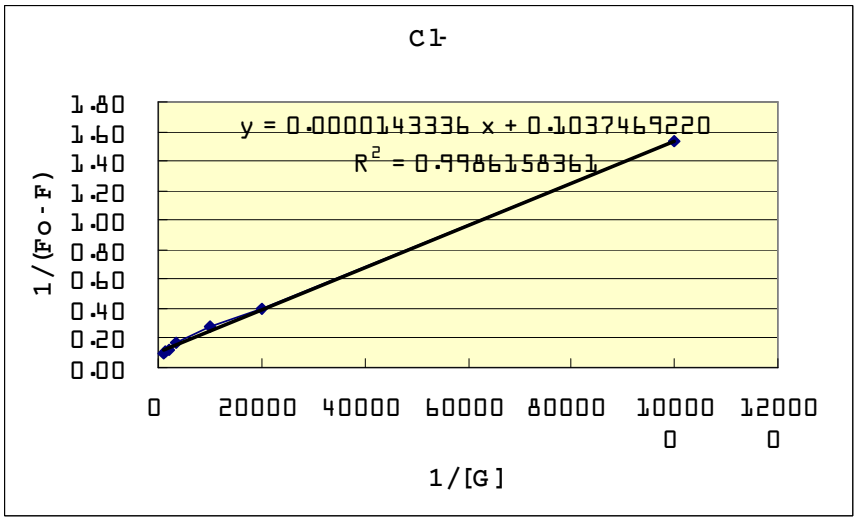

$K_a = 7238.02\ M^{-1}$

S-Figure 24. (a) Fluorescent titration spectra of **1** (10 μM) upon addition of Chloride ion in 100 % CH_3CN (excitation: 360 nm). (b) Benesi-Hildebrand plot of emission spectra of **1** at 360 nm: [1 / (F_0-F)] / [G].

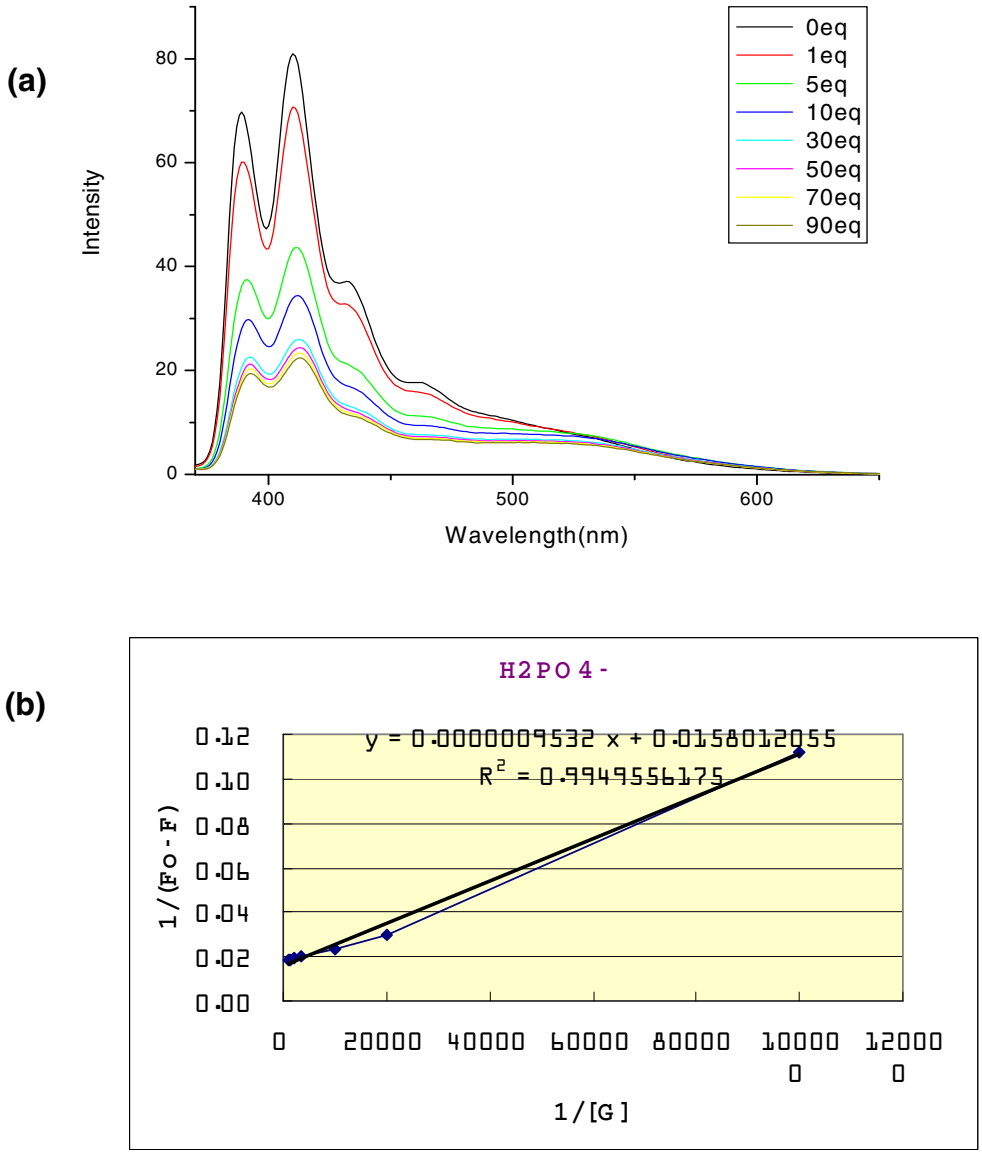

$K_a = 16577.01\ M^{-1}$

S-Figure 25. (a) Fluorescent titration spectra of **2** (10 μM) upon addition of $H_2PO_4^-$ ion in 100 % CH_3CN (excitation: 360 nm). (b) Benesi-Hildebrand plot of emission spectra of **2** at 360 nm: [1 / (F_0-F)] / [G].

(a)

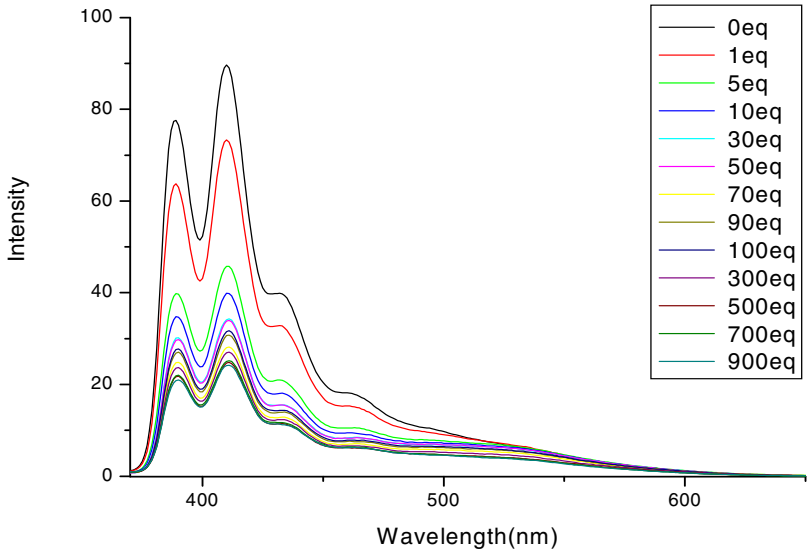

(b)

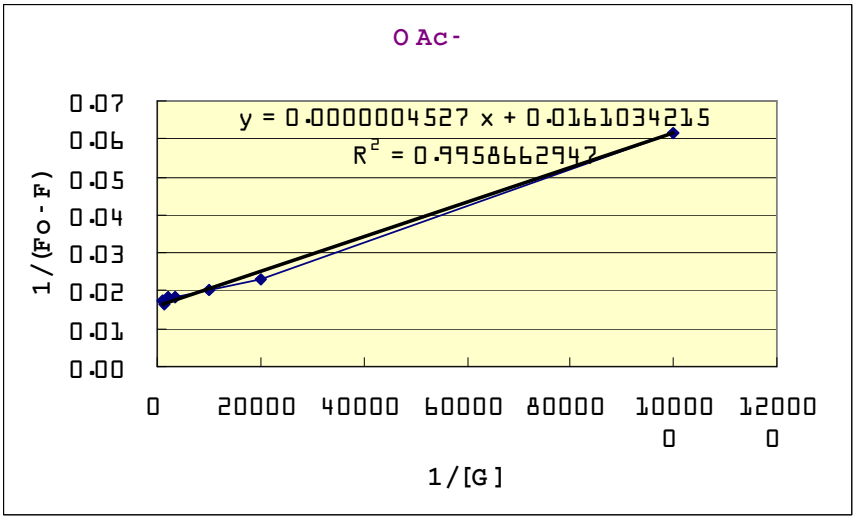

$K_a = 35571.95\ M^{-1}$

S-Figure 26. (a) Fluorescent titration spectra of **2** (10 μM) upon addition of CH_3COO^- ion in 100 % CH_3CN (excitation: 360 nm). (b) Benesi-Hildebrand plot of emission spectra of **2** at 360 nm : [1 / (F_0-F)] / [G].

Theoretical Calculations

Density functional B3LYP/6-31G* calculations were used for the geometry optimization for host **1** and D/L-t-Boc-alanine complexes. In the case of host **2** and D/L-t-Boc-alanine complexes, certain parts of the host 2 and D/L amino acids were considered with high levels of calculation (MP2/6-31G*) in order to define the H-π interactions appropriately; hence, we used ONIOM (MP2/6-31G*+B3LYP/6-31G*) based calculation for the geometry optimization. RIMP2/cc-pVDZ single point calculated energies on the ONIOM optimized geometries were used for the total energy comparison between the **2**-D-t-Boc-alanine complex and the **2**-L-t-Boc-alanine complex. The contribution of the H-π interaction toward the total energy was calculated by considering the interaction between the anthracene moiety and two methyl moieties extracted from the ONIOM optimized geometries. Energies of the H-π interacted moieties in acetonitrile were calculated with Isodensity surface polarized continuum model (IPCM) at the MP2/6-31G* level.

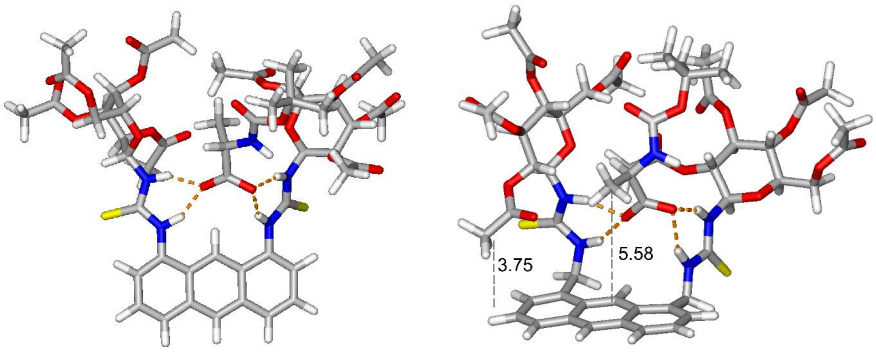

a) **b)**

S-Figure 27. Optimized geometries of a) **1**-L-*t*-Boc-alanine complex [at the B3LYP/6-31G* level], and b) **2**-D-*t*-Boc-alanine complex [at the ONIOM (MP2/6-31G*+B3LYP/6-31G*) level]

In both the optimized geometries of **2**-D-*t*-Boc-alanine and **2**-L-*t*-Boc-alanine complexes, we observed that the distance from the methyl carbon atom of -CH_2-OAc in glucopyranosyl group to the anthracene plane is not significantly different from each other (3.75 Å vs. 3.63 Å). However, there is a significant difference in the distance from the methyl carbon atom of D-*t*-Boc-alanine/L-*t*-Boc-alanine to the anthracene plane (5.58 Å/4.15 Å). This is in agreement with the chemical shift changes observed for the H-atoms of the methyl group of D-*t*-Boc-alanine/L-*t*-Boc-alanine.

References

[1] Kwon, J. Y.; Jang, Y. J.; Kim, S. K.; Lee, K. H.; Kim, J. S.; Yoon, J. *J. Org. Chem.* **2004**,

69(15), 5155-5157.

[2] Kim, S. K.; Yoon, J. *Chem. Commun*. **2002,** 770-771**.**